RSC Advances

PAPER

Cite this: *RSC Adv.*, 2020, **10**, 26262

Polymer wrapping-induced dispersion of single walled carbon nanotubes in ethylene glycol under mild sonication†

Dukeun Kim,‡[a] Taeheon Lee,‡[b] Minho Kwon,[b] Hyun-jong Paik,*[b] Jong Hun Han,[c] Min Kang,[a] Jueun Choi,[a] Seungki Hong[ad] and Yoong Ahm Kim*[a]

Received 5th May 2020
Accepted 3rd July 2020

DOI: 10.1039/d0ra04061d

rsc.li/rsc-advances

SWCNTs were individually dispersed in ethylne glycol (EG) *via* mild bath-type sonication using quaternized poly(furfuryl methacrylate)-*co*-(2-(dimethylamino)ethyl methacrylate) p(FMA-*co*-QDMAEMA) as a dispersing agent. QDMAEMA, which has alkyl groups, was more favorable to the dispersion ability of single walled carbon nanotubes (SWCNTs). The dispersion mechanism of SWCNTs in EG *via* helical wrapping of polymer chains along their sidewalls was suggested based on transmission electron microscopic observation.

The preparation process for stable single walled carbon nanotube (SWCNT) suspensions[1,2] is considered one of the most important steps for utilization in various promising applications, such as transistors,[3,4] solar cells,[5,6] bio/chemical[7,8] and optical sensors,[9,10] electronics,[11,12] and polymer reinforcements.[13,14] As-synthesized SWCNTs exhibit a large bundled structure and are insoluble both in water and in common organic solvents because of the strong polarizability induced by their unique structure and strong van der Waals binding energy (~500 eV) between the tubes.[15,16] These properties limit the processability of SWCNTs, thereby restricting their usage in several promising applications. Various approaches have been proposed to produce stable dispersions of individual SWCNTs in several solvents through noncovalent functionalization. These approaches utilize adsorbing agents, for example, a surfactant[17,18] and an organic polymer,[19,20] which possess high dissolving properties in water or in organic solvents. However, such approaches cannot occur spontaneously. High energy generated from ultra-sonication is usually employed to achieve interaction between SWCNTs and adsorbing agents, thereby resulting in de-bundled or dispersed SWCNTs. Despite these efforts, stable SWCNT dispersions are still difficult to produce because the mechanism and important factors that influence optimal synthesis are not well understood.

To clearly determine the important factors for preparing SWCNT suspensions, input of less energy into the SWCNT solution is highly desirable[21–24] because long, less defective, and individualized tubes are critically needed in various applications. In our previous reports,[21,23] we synthesized polymeric dispersants that are able to disperse SWCNTs in organic solvents using a bath-type sonicator. More specifically, stable SWCNT suspensions in organic solvents were produced under mild bath-type sonication using quaternized poly(furfuryl methacrylate)-*co*-(2-(dimethylamino)ethyl methacrylate) (p(FMA-*co*-QDMAEMA)) with a low percentage of QDMAEMA, which acts as a solubility-improving group (stabilizer).[21] However, there is no systematic study on the effect of polymeric compositions on the dispersion state of SWCNTs and the manner in which bundled SWCNTs are disentangled and then individualized in ethylene glycol (EG).

Herein, we synthesized p(FMA-*co*-QDMAEMA) with two different compositions (FMA : QDMAEMA = 7 : 3 (denoted p(F7QD3) and = 3 : 7 (denoted p(F3QD7)) and then evaluated them as dispersing agents for strongly bundled SWCNTs in EG. SWCNT suspensions using p(F7QD3) and p(F3QD7) in EG were evaluated in terms of their dispersability using several optical tools. Because fluorescence of SWCNTs can be only observed when the SWCNTs are present as individuated semiconducting nanotubes, such property can be utilized not only to confirm the dispersion and disentanglement of SWCNTs, but also to investigate their optical properties. Furthermore, the dispersion

[a]*Department of Polymer Engineering, Graduate School, School of Polymer Science and Engineering, Alan G. MacDiarmid Energy Research Institute, Chonnam National University, 77 Yongbong-ro, Buk-gu, Gwangju 61186, Republic of Korea. E-mail: yak@chonnam.ac.kr*

[b]*Department of Polymer Science and Engineering, Pusan National University, San 30 Jangion2 dong, Geumjeong-gu, Busan 609-735, Republic of Korea. E-mail: hpaik@pusan.ac.kr*

[c]*School of Chemical Engineering, Optoelectronics Convergence Research Center, Chonnam National University, 77 Yongbong-ro, Buk-gu, Gwangju 61186, Republic of Korea*

[d]*Carbon Composite Material Research Center, Korea Institute of Science and Technology (KIST), Jeonbuk 55324, Republic of Korea*

† Electronic supplementary information (ESI) available: NMR spectra, XPS analysis, and GPC. See DOI: 10.1039/d0ra04061d

‡ Both authors contributed to this work equally.

mechanism of bundled SWCNTs in EG *via* the wrapping of polymeric dispersant was proposed based on detailed TEM observation.

Experimental

Materials

Hipco-based single walled carbon nanotubes (SWCNTs, Nano Integris) were purchased. Furfuryl methacrylate (FMA, 97%, Sigma-Aldrich) and 2-(dimethylamino) ethyl methacrylate (DMAEMA, 98%, TCI) were purified using an alumina column to remove inhibitors before use. Copper(I) bromide (CuBr, 99%, Sigma-Aldrich) was purified according to a published procedure.[21,23] Ethyl 2-bromoisobutyrate (EBiB, 99%, Sigma-Aldrich), 4,4-dinonyl-2,2-bipyridyl (dNbpy, 97%, Sigma-Aldrich), Iodomethane (99%, Sigma-Aldrich), tetrahydrofuran (THF, 99.8%, J. T. Baker), dimethylformamide (DMF, 99.5%, TCI chemicals), and ethylene glycol (EG, 99.5%, TCI chemicals) were used as received.

Synthesis of polymeric dispersant

The syntheses of p(FMA-*co*-QDMAEMA) with various compositions, *i.e.*, FMA : QDMAEMA = 7 : 3 (denoted p(F7QD3)), and 3 : 7 (denoted p(F3QD7)), were performed from quaternization of p(FMA-DMAEMA) synthesized by atom transfer radical polymerization (ATRP) (Scheme 1). Then, p(FMA-*co*-DMAEMA) was synthesized[23] as follows: DMAEMA (0.51 mL, 3.07 mmol for p(F7QD3) or 1.03 mL, 6.13 mmol for p(F3QD7)), FMA (0.95 mL, 6.13 mmol for p(F7QD3) or 0.47 mL, 3.07 mmol for p(F3QD7), FMA (0.95 mL, 6.13 mmol for p(F7QD3) or 0.47 mL, 3.07 mmol for p(F3QD7)), EBiB (10 μm, 6.81×10^{-2} mmol), and anisole were added to a Schlenk flask after deoxygenation by bubbling with N_2 for 30 min. Three cycles of vacuum and filling with nitrogen were repeated. After freezing the solution, dNbpy (55.7 mg, 13.6×10^{-2} mmol) and CuBr (9.77 mg, 6.81×10^{-2} mmol) were added, the flask was sealed with a glass stopper, and the cycle of vacuum and filling with nitrogen was repeated three times. The solution was submerged into an oil bath at 50 °C. After polymerization, the solution was diluted with THF and passed through a neutral alumina column to remove the copper catalyst. The final product, p(FMA-*co*-DMAEMA), was isolated from hexane. The product was finally dried under vacuum at room temperature (M_n = 14 800 and PDI = 1.42 of p(F7QD3) and M_n = 17 000, PDI = 1.34 of p(F3QD7), respectively, were determined by GPC, Fig. S2(a)†). The compositions of the individual monomer in the polymer chain were confirmed by 1H NMR. The ratio of integration of peaks from furan group at δ = 7.4 ppm and methylene ($-CO_2CH_2-$) group at δ = 4.02 ppm were used to calculate composition of each monomer in polymer chain. Subsequently, p(FMA-*co*-DMAEMA) was quaternized to produce p(FMA-*co*-QDMAEMA) as follows: 0.5 g of p(FMA-*co*-DMAEMA) was dissolved in DMF (2 mL) with stirring at room temperature.[21] Iodomethane (0.2 mL, 3.21 mmol) was added, and the mixture was then stirred for 24 h. The quaternized polymer was precipitated in isopropyl ether, followed by drying under vacuum for 48 h. The quaternization of amine in DMAEMA moiety was confirmed by peak shift in 1H NMR for p(FMA-*co*-QDMAEMA). After quaternization of amine, the methylene ($-CO_2CH_2-$) proton peak of DMAEMA moiety which appeared at δ = 4.02 ppm in p(FMA-*co*-DMAEMA) shifts to δ = 4.34 ppm in p(FMA-*co*-QDMAEMA) (Fig. S2(b) and (c)†).

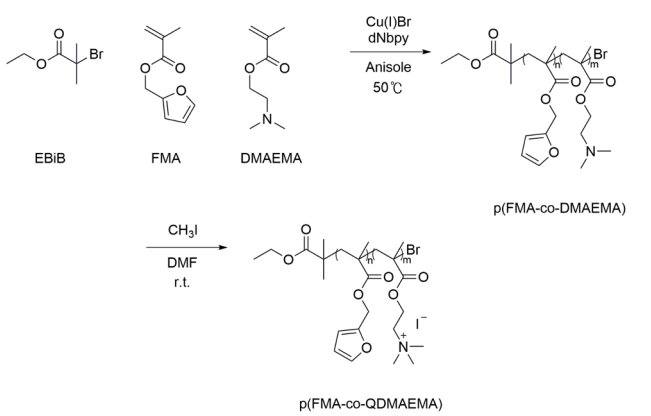

Scheme 1 Synthesis of polymeric dispersant, p(FMA-*co*-QDMAEMA), by combination of ATRP and quaternization of DMAEMA in the polymer chain.

Dispersion of SWCNTs using polymeric dispersants

The polymeric p(F7QD3) and p(F3QD7) (20 mg) were dissolved in EG solution (20 mL). SWCNTs (2 mg) were added to the polymer solutions and the polymer solutions containing SWCNTs were sonicated using a bath-type sonicator (Branson 3210, Branson Ultrasonics Corp., USA) for 3 h. The sonicated solutions were centrifuged at 100 000*g* for 30 min (Optima™ MAX-XP Ultracentrifuge, Beckman Coulter Inc.) to remove bundled nanotubes. Stable SWCNT suspensions in EG were obtained as the supernatant.

Characterization

The number average molecular weight (M_n) and the polydispersity index (PDI) were confirmed using gel permeation chromatography (GPC), which was calibrated using poly(methyl methacrylate) as a standard material. The chromatograph was equipped with an Agilent 1100 pump, a RID detector, and PSS SDV (5 μm; 105, 103, and 102 Å; 8.0 × 300.0 mm) columns. The synthesized polymeric dispersants were investigated by 1H-NMR spectroscopy (Varian Unity Inova-500, Oxford) in chloform-d or DMF-d7 as a solvent. The polymer dispersed SWCNT suspensions were characterized by UV-vis-NIR (solidspec-3700, Shimadzu Ltd., Japan), Multidimensional liquid-NIR laser Raman (InVia Reflex, Renishaw Ltd., U.K.), photoluminescence (PL, NIR-PL system, Shimadzu Ltd., Japan) mapping, and TEM (Titan 80–300™, FEI Ltd., USA). Raman spectra were measured using a 785 nm laser line. The X-ray photoelectron spectroscopy (XPS) spectra were recorded on a Thermo Scientific, ESCALAB 250Xi XPS spectrometer.

Results and discussions

The SWCNT suspensions were obtained using p(F7QD3) and p(F3QD7) in EG under mild bath-type sonication and

a subsequent centrifugation process. A homogeneous dark-black solution was formed without any floating particles. The transparency of SWCNT suspensions obviously differed depending on the composition of the polymeric dispersants, indicating that the opacity of SWCNT suspensions produced using p(F3QD7) was clearly higher than those using p(F7QD3) (Fig. 1(a)). Typically, non-covalent dispersion of nanotubes *via* the adsorption of polymer is achieved through π–π interaction between the sidewall of tubes and the aromatic groups of polymers.[24] The density of functional groups within the polymer affects the dispersion state of SWCNTs in various solvents.[24] In this respect, direct comparison between SWCNT suspensions obtained using p(F3QD7) and p(F7QD3) allow us to conclude that the density of quaternized groups contributed to the dispersion of SWCNTs in EG, even though the adsorbing force onto the nanotubes' sidewalls was slightly weak. Thus, to identify the presence of polymeric dispersants on the sidewalls of tubes, the black powder was obtained by filtering SWCNT suspensions and was then characterized using XPS (Fig. S1†). In the C 1s XPS spectrum of pristine SWCNTs, we clearly observed a strong peak at 284.5 eV corresponding to sp^2-hybridized carbon. Two peaks, at 285.8 and 289.4 eV, respectively, corresponding to oxygen functional groups, such as CO and C=O peaks, were identified as part of the oxidative purification process. When polymeric dispersants are introduced to SWCNTs, the –CO– and –C=O peaks were shifted to 285.6 and 288.3 eV, respectively, and new oxygen peaks corresponding to ketone and C–O were confirmed at 532.4 and 534.2 eV, respectively. Thus, we are able to say that polymeric dispersants were securely attached to the sidewalls of SWCNTs, thereby resulting in the dispersion of tubes in EG. Moreover, understanding the solvent effect when obtaining the SWCNT suspension is important because solvents with prominent dipole moments, such as DMF, EG, and pyridine, can play a vital role in the dispersion of nanotubes.[25] Thus, the zeta potential of the SWCNT suspensions obtained using the two different polymeric dispersants was measured in solution phase. Understandably, the quaternized groups can allow the polymer dispersants to have a positive charge, thus leading to electrostatic repulsion between the disentangled nanotubes. The zeta-potential values of SWCNT suspensions using p(F7QD3) and p(F3QD7) were +82.27 mV and +52.57 mV, respectively. Even though p(F3QD7) has a higher percentage of quaternized groups, the zeta-potential value of the p(F3QD7)/SWCNT suspension was relatively lower than that of the p(F7QD3)/SWCNT one. Because of anchoring function of FMA moiety, the amount of adsorbed p(F3QD7) per unit area of SWCNTs might be smaller than that of p(F7QD3), thereby resulting in the reduced surface potential. Considering the value of zeta potential, the two polymeric dispersant-SWCNT suspensions exhibit high zeta potential value above 40 mV,[26] indicating the high dispersion and disentanglement ability of the polymeric dispersants.

To compare the dispersability of the two polymeric dispersants with respect to the pristine SWCNTs in EG quantitatively,

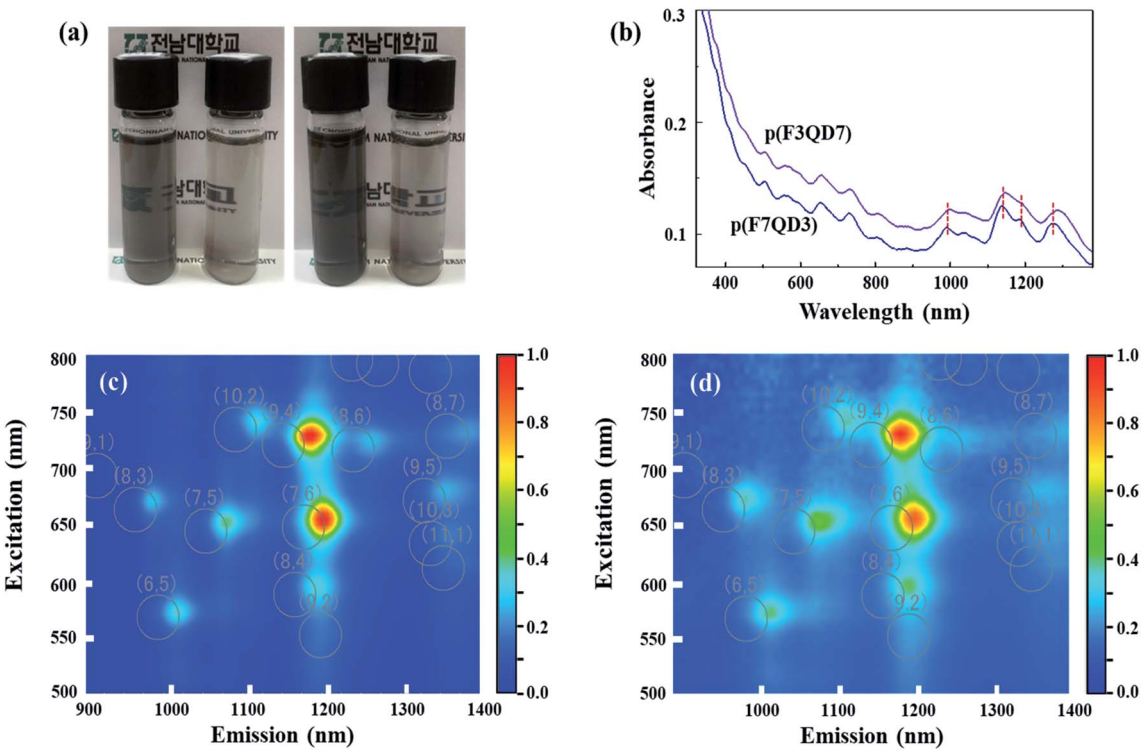

Fig. 1 (a) Photographic images showing SWCNT suspensions in ethylene glycol before and after centrifugation using (left) p(FMA-*r*-QDMAEMA) ($n = 68$, $m = 34$) (denoted p(F7QD3)), (right) p(FMA-*r*-QDMAEMA) ($n = 25$, $m = 74$) (denoted p(F3QD7)). (b) UV-vis-NIR spectra and photoluminescence maps of SWCNT suspensions in ethylene glycol using (c) p(F7QD3) and (d) p(F3QD7). The colour represents the photoluminescence intensity on a linear scale.

UV-vis-NIR absorption spectra were obtained for polymer-dispersed SWCNT suspensions (Fig. 1(a)). The clearly resolved optical peaks in S_{11} (approximately 830–1600 nm), S_{22} (approximately 600–830 nm), and M (approximately 600–440 nm) indicate that SWCNTs were individualized,[27] even though it is difficult to determine clear metallic and/or semiconducting sharp peaks because of the overlapped polymer absorbance. From the UV absorption spectra, it is clear that mild bath-type sonication is able to obtain individualized SWCNTs in EG *via* the adsorption of polymers on the tubes' sidewalls. A distinctive blue-shift of the absorbance peaks in S_{11} for the p(F3QD7)-dispersed SWCNT suspension when compared with that of the p(F7QD3)-dispersed SWCNT one can be explained by the complicated chiralities of dispersed SWCNTs in EG. Because the absorbance intensity is dependent on the amount of dispersed nanotubes, the higher absorbance for the p(F3QD7)-dispersed SWCNT suspension indicates that p(F3QD7) has higher dispersability than p(F7QD3). Moreover, to understand the effect of the adsorbed polymers on the optical properties of SWCNT suspensions, we obtained PL maps from two SWCNT suspensions (Fig. 1(c)) because photoluminescence is a powerful tool to analyze individualized semiconducting SWCNTs.[28] The observation of two strong PL peaks (corresponding to semiconducting SWCNTs with chiralities (9,4) and (7,6)) signifies that the SWCNTs were individually dispersed by attaching p(F7QD3) and p(F3QD7) to the nanotubes' sidewall in EG, even though we employed a mild bath-type sonicator. As compared with sodium dodecyl benzenesulfonate (SDBS)-dispersed SWCNT suspensions (white circles in Fig. 1(c)),[10,29,30] the noticeable red-shift in excitation from polymer dispersant-dispersed SWCNT suspensions can be explained by environmental dielectric screening effects.[31]

To characterize the dispersion state of SWCNTs with the help of polymeric dispersant in detail, we acquired Raman spectra using a 785 nm laser line before and after bath-type sonication (Fig. 2). The pristine SWCNTs displayed several radial breathing modes (RBMs, which correspond to a coherent vibration of the carbon atoms normal to the tube axis) below 500 cm^{-1}, a weak D-band (defect induced mode) at approximately 1300 cm^{-1}, a strong G-band (E_{2g2} mode) at 1600 cm^{-1}, and a G′-band at ~2600 cm^{-1}. When sonicating the pristine SWCNTs in EG without the addition of polymer, the observation of both a weak G band from SWCNTs and several strong Raman peaks from EG indicates the low dispersability of EG with respect to the bundled SWCNTs. However, for the bath-sonicated SWCNT suspension prepared with the addition of polymeric dispersant, the observation of both G and strong luminescent peaks indicates the presence of individually dispersed SWCNTs in EG. Because the RBMs of SWCNTs observed below 500 cm^{-1} are sensitive to their diameter and bundled state,[32–34] we enlarged the low-frequency RBMs (see insets in Fig. 2). Each peak represents specific nanotubes and provides some insight into the observed change. In particular, the intensity of the peak at 267 cm^{-1}, related to the (10,2) nanotube, decreases when SWCNTs are homogeneously dispersed.[32] Therefore, the polymer used in this work exhibited high dispersability with respect to the strongly bundled

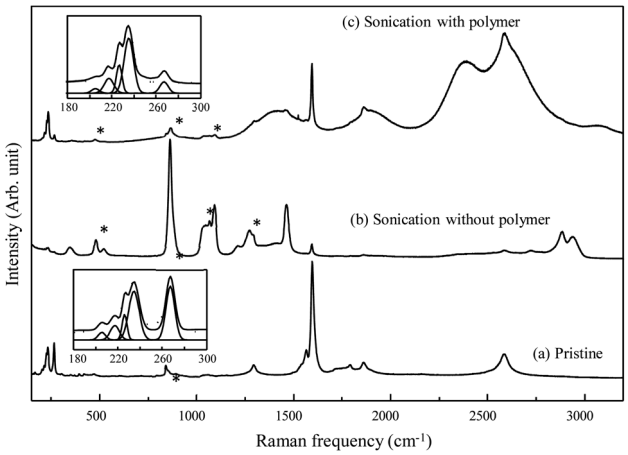

Fig. 2 Raman/fluorescence spectra using a 785 nm laser line for (a) pristine SWCNTs and for SWCNTs in ethylene glycol under a bath-type sonicator (b) without and (c) with polymeric dispersant. The insets show magnified low-frequency Raman spectra for the corresponding samples. Solvent peaks were marked with asterisks.

SWCNTs in EG, especially using mild bath-type sonication. Moreover, to determine the dispersability of the polymer dispersants with various compositions in EG, Raman/fluorescence spectra of two supernatant obtained using different polymers were directly compared (Fig. 3). Both suspensions exhibited five strong luminescent peaks, corresponding to (6,4), (9,1), (8,3), (6,5) and (7,5) chiralities, respectively. The clear observation of strong luminescent peaks indicates the presence of individual SWCNTs in EG. As described in the experimental section, the supernatant was obtained using ultracentrifugation to remove thin bundled SWCNTs. Therefore, ultracentrifugation increases the intensity of the luminescence peaks. We also observed brighter luminescence peaks for the p(F3QD7)-dispersed SWCNT suspension compared with those of the p(F7QD3)-dispersed

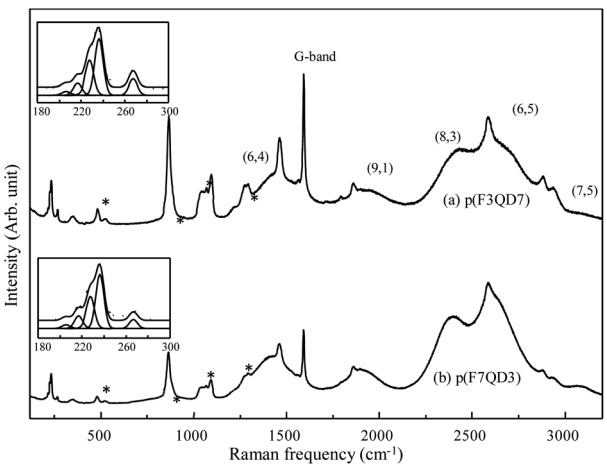

Fig. 3 Comparative Raman/fluorescence spectra using a 785 nm laser line for p(F3QD7)- and p(F7QD3)-dispersed SWCNT supernatants. The insets show the magnified low-frequency Rama spectra for the corresponding samples. Solvent peaks were marked with asterisks.

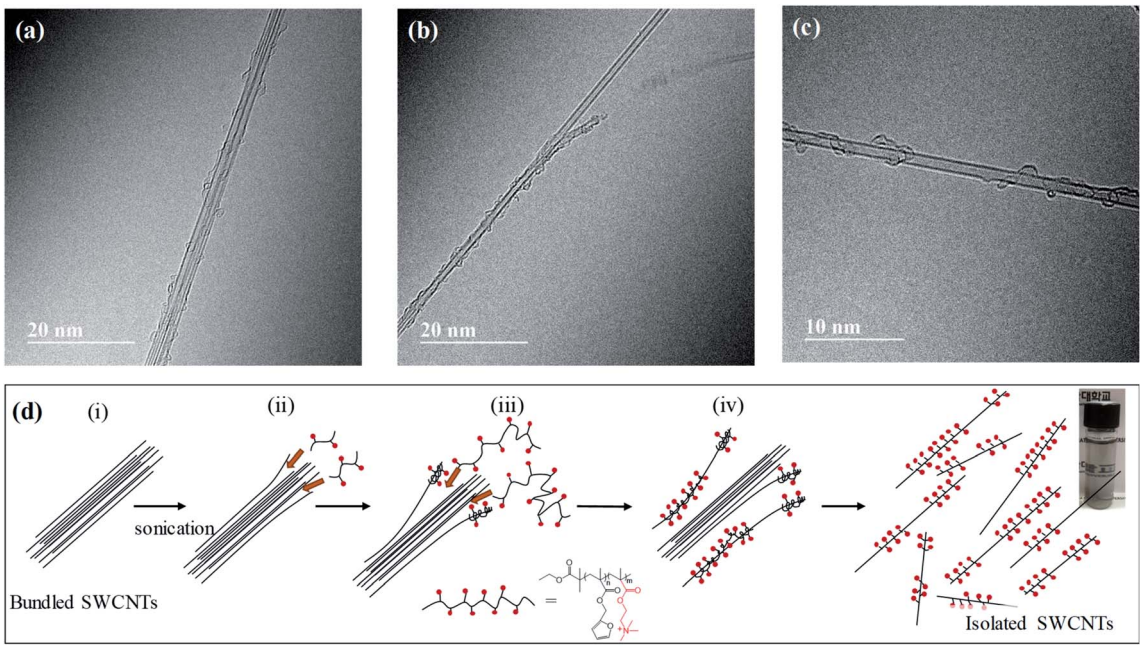

Fig. 4 Transmission electron microscopy images showing the dispersion state of SWCNTs *via* polymer wrapping: (a) small-sized bundle, (b) separation point of small-sized bundle, (c) an individualized SWCNT, and (d) suggested dispersion mechanism of SWCNTs from bundles *via* wrapping of polymer chains.

SWCNT suspension. This result indicates that p(F3QD7) has higher dispersability than p(F7QD3) with respect to bundled SWCNTs in EG. In addition, no distinctive difference between the RBMs of the two suspensions is observed, but the intensity of the RBMs for the p(F3QD7)-dispersed SWCNT suspension is two times that of the p(F7QD3)-dispersed SWCNT suspension.

Finally, to understand how the polymer disperses SWCNTs in EG, we carried out detailed TEM observation of the p(F3QD7)-dispersed SWCNT suspension. We observed small-sized SWCNT bundles (Fig. 4(a)), detached SWCNTs from bundled SWCNTs (Fig. 4(b)), and an individual SWCNT (Fig. 4(c)). It is interesting to note that polymer chains are helically wrapped along the sidewalls of the SWCNTs. TEM observation allows us to suggest a possible dispersion mechanism for SWCNT suspensions *via* helical wrapping of a polymer chain on the sidewall of SWCNTs in EG under mild bath-type sonication (Fig. 4(c)). Several previous studies[35–37] reported that the outermost tubes of a SWCNT bundle could be more easily detached than the innermost tubes, in which the outer tubes tended to disentangle from the bundle ends. Therefore, prior to interaction with the polymeric dispersant, mechanical disentanglement of bundles should be accomplished by sonication. Sonication provides local shear force, particularly to the nanotube bundle ends ((i) in Fig. 4(c)). Once a tiny space or gap is formed at the bundle ends, dispersants with small molecular weight are probably adsorbed at the ends ((ii) in Fig. 4(c)). Because of electrostatic repulsion[21] between the dispersant-adsorbed bundle ends, greater spaces or gaps can be produced. Naturally, polymeric dispersants with large molecular weight can be adsorbed to wrap along the sidewall of the SWCNT ((iii) in Fig. 4(c)), which eventually leads to nanotubes completely separated from bundles ((iv) in Fig. 4(c)).

Conclusions

We demonstrated the ability to produce SWCNT suspensions in EG with the help of polymeric dispersants composed of FMA and QDMAEMA with different compositions using mild bath-type sonication. It is clear that the structure and composition ratio of polymeric dispersants determined the dispersion state of SWCNTs in EG. According to various optical characterizations, p(F3QD7), which has a high percentage of alkyl groups, exhibited higher dispersability for SWCNTs than did p(F7QD3). The dispersion procedure of SWCNTs *via* helical wrapping of polymer chains along their sidewalls was suggested based on TEM observation; (1) sonication induced the formation of gaps or spaces at the bundle ends; (2) the dispersants with low molecular weight probably penetrated into these spaces; (3) the isolation of nanotubes from bundles progressed utilizing another dispersant having high molecular weight; (4) ultimately producing a disentangled nanotube.

Conflicts of interest

There are no conflicts to declare.

Acknowledgements

Y. A. K. acknowledges financial support from an NRF grant funded by the Korea government (MSIP) (No. 2017R1A2A1A17069771 and 2017M3A7B4014045). J. H. H. acknowledges financial support from Priority Research Centers Program through the National Research Foundation of Korea (NRF) funded by the Ministry of Education, Science and Technology (2018R1A6A1A03024334) and Industrial Fundamental

Technology Development Program (10052838) funded by the Ministry of Trade, Industry and Energy (MOTIE).

Notes and references

1 G. S. Demirer, H. Zhang, J. L. Matos, N. S. Goh, F. J. Cunningham, Y. Sung, R. Chang, A. J. Aditham, L. Chio, M.-J. Cho, B. Staskawicz and M. P. Landry, *Nat. Nanotechnol.*, 2019, **14**, 456–464.

2 B. Cheng, S. Yang, Y. T. Woldu, S. Shafique and F. Wang, *Nanotechnology*, 2020, **31**, 145707.

3 C. Cao, J. B. Andrews, A. Kumar and A. D. Franklin, *ACS Nano*, 2016, **10**, 5221–5229.

4 H. Gui, H. Chen, C. Y. Khripin, B. Liu, J. A. Fagan, C. Zhou and M. Zheng, *Nanoscale*, 2016, **8**, 3467–3473.

5 U. Kumar, S. Sikarwar, R. K. Sonker and B. C. Yadav, *J. Inorg. Organomet. Polym.*, 2016, **26**, 1231–1242.

6 S.-H. Lee, S.-J. Ko, S. H. Eom, H. Kim, D. W. Kim, C. Lee and S. C. Yoon, *ACS Appl. Mater. Interfaces*, 2020, **12**, 14244–14253.

7 N. T. Tung, P. T. Tue, T. Thi Ngoc Lien, Y. Ohno, K. Maehashi, K. Matsumoto, K. Nishigaki, M. Biyani and Y. Takamura, *Sci. Rep.*, 2017, **7**, 17881.

8 V. Schroeder, S. Savagatrup, M. He, S. Lin and T. M. Swager, *Chem. Rev.*, 2019, **119**, 599–663.

9 R. M. Williams, C. Lee and D. A. Heller, *ACS Sens.*, 2018, **3**, 1838–1845.

10 E. Turek, T. Shiraki, T. Shiraishi, T. Shiga, T. Fujigaya and D. Janas, *Sci. Rep.*, 2019, **9**, 535.

11 S. Park, M. Vosguerichian and Z. Bao, *Nanoscale*, 2013, **5**, 1727–1752.

12 W. J. Yu, S. Y. Lee, S. H. Chae, D. Perello, G. H. Han, M. Yun and Y. H. Lee, *Nano Lett.*, 2011, **11**, 1344–1350.

13 N. Salah, A. M. Alfawzan, A. Saeed, A. Alshahrie and W. Allafi, *Sci. Rep.*, 2019, **9**, 20288.

14 M. Heidarshenas, M. Kokabi and H. Hosseini, *Polym. J.*, 2019, **51**, 579–590.

15 C. Pramanik, J. R. Gissinger, S. Kumar and H. Heinz, *ACS Nano*, 2017, **11**, 12805–12816.

16 H. Cui, X. Yan, M. Monasterio and F. Xing, *Nanomaterials*, 2017, **7**, 262.

17 E. Ramos, W. A. Pardo, M. Mir and J. Samitier, *Nanotechnology*, 2017, **28**, 135702.

18 F. Ernst, Z. Gao, R. Arenal, T. Heek, A. Setaro, R. Fernandez-Pacheco, R. Haag, L. Cognet and S. Reich, *J. Phys. Chem. C*, 2017, **121**, 18887–18891.

19 Y. Zhang, B. R. Bunes, C. Wang, N. Wu and L. Zang, *Sens. Actuators, B*, 2017, **247**, 713–717.

20 C. Liang, B. Wang, J. Chen, Q. Yong, Y. Huang and B. Liao, *J. Phys. Chem. B*, 2017, **121**, 8408–8416.

21 T. Lee, J. Park, K. Kim, A. K. Mohanty, B. Kim, J. H. Han, H. B. Jeon, Y. S. Lee and H.-j. Paik, *RSC Adv.*, 2015, **5**, 69410–69417.

22 C.-Y. Hu, Y.-J. Xu, S.-W. Duo, R.-F. Zhang and M.-S. Li, *J. Chin. Chem. Soc.*, 2009, **56**, 234–239.

23 T. Lee, B. Kim, S. Kim, J. H. Han, H. B. Jeon, Y. S. Lee and H.-j. Paik, *Nanoscale*, 2015, **7**, 6745–6753.

24 B.-S. Kim, D. Kim, K.-W. Kim, T. Lee, S. Kim, K. Shin, S. Chun, J. H. Han, Y. S. Lee and H.-j. Paik, *Carbon*, 2014, **72**, 57–65.

25 K. D. Ausman, R. Piner, O. Lourie, R. S. Ruoff and M. Korobov, *J. Phys. Chem. B*, 2000, **104**, 8911–8915.

26 M. Khan, A. Shakoor, G. Khan, S. Sultana and A. Zia, *J. Chem. Soc. Pak.*, 2015, **37**, 62–67.

27 S. Attal, R. Thiruvengadathan and O. Regev, *Anal. Chem.*, 2006, **78**, 8098–8104.

28 S. M. Bachilo, M. S. Strano, C. Kittrell, R. H. Hauge, R. E. Smalley and R. B. Weisman, *Science*, 2002, **298**, 2361–2366.

29 V. Strauss, J. T. Margraf, T. Clark and D. M. Guldi, *Chem. Sci.*, 2015, **6**, 6878–6885.

30 J. Sim, S. Kim, M. Jang, M. Park, H. Oh and S.-Y. Ju, *Langmuir*, 2017, **33**, 11000–11009.

31 O. A. Dyatlova, J. Gomis-Bresco, E. Malic, H. Telg, J. Maultzsch, G. Zhong, J. Geng and U. Woggon, *Phys. Rev. B: Condens. Matter Mater. Phys.*, 2012, **85**, 245449–245454.

32 D. A. Heller, P. W. Barone, J. P. Swanson, R. M. Mayrhofer and M. S. Strano, *J. Phys. Chem. B*, 2004, **108**, 6905–6909.

33 P. T. Araujo, C. Fantini, M. M. Lucchese, M. S. Dresselhaus and A. Jorio, *Appl. Phys. Lett.*, 2009, **95**, 261902–261904.

34 A. Jorio, A. P. Santos, H. B. Ribeiro, C. Fantini, M. Souza, J. P. M. Vieira, C. A. Furtado, J. Jiang, R. Saito, L. Balzano, D. E. Resasco and M. A. Primenta, *Phys. Rev. B: Condens. Matter Mater. Phys.*, 2005, **72**, 075207–075211.

35 M. S. Strano, V. C. Moore, M. K Miller, M. J Allen, E. H. Haroz, C. Kittrell, R. H. Hauge and R. E. Smalley, *J. Nanosci. Nanotechnol.*, 2003, **3**, 81–86.

36 X. Xin, G. Xu and H. Li, in *Physical and Chemical Properties of Carbon Nanotubes*, ed. S. Suzuki, InTech, Rijeka, 1st edn, 2013, ch. 10, vol. 1, pp. 245–263.

37 W. Wenseleers, I. I. Vlasov, E. Goovaerts, E. D. Obraztsova, A. S. Lobach and A. Bouwen, *Adv. Funct. Mater.*, 2004, **14**, 1105–1112.